Available online at www.sciencedirect.com
ScienceDirect
International Journal of Mass Spectrometry 270 (2008) 139–155
International Journal of Mass Spectrometry
www.elsevier.com/locate/ijms

Knudsen effusion mass spectrometric determination of mixing thermodynamic data of liquid Ag–In–Sn alloy

L. Bencze [a,*], A. Popovic [b]

[a] *Eötvös Loránd University, Department of Physical Chemistry, H-1117 Budapest, Pázmány Péter sétány 1/A, Hungary*
[b] *Jozef Stefan Institute, Jamova 39, SLO-1000 Ljubljana, Slovenia*

Received 19 October 2007; received in revised form 7 December 2007; accepted 7 December 2007
Available online 23 December 2007

Abstract

The vaporisation of a liquid Ag–In–Sn system has been investigated at 1273–1473 K by Knudsen effusion mass spectrometry (KEMS) and the data fitted to a Redlich–Kister–Muggianu (RKM) sub-regular solution model. Nineteen different compositions have been examined at six fixed indium mole fractions, $X_{In} = 0.10$, 0.117, 0.20, 0.30, 0.40 and 0.50. The ternary *L*-parameters, the thermodynamic activities and the thermodynamic properties of mixing have been evaluated using standard KEMS procedures and from the measured ion intensity ratios of Ag^+ to In^+ and Ag^+ to Sn^+, using a mathematical regression technique described by us for the first time. The intermediate data obtained directly from the regression technique are the RKM ternary *L*-parameters. From the obtained ternary *L*-parameters the integral molar excess Gibbs free energy, the excess chemical potentials, the activity coefficients and the activities have been evaluated. Using the temperature dependence of the activities, the integral and partial molar excess enthalpies and entropies were determined. In addition, for comparison, for some compositions, also the Knudsen effusion isothermal evaporation method (IEM) and the Gibbs–Duhem ion intensity ratio method (GD-IIR) were used to determine activities and good agreement was obtained with the data obtained from fitting to the RKM model.

Keywords: Knudsen effusion mass spectrometry; Redlich–Kister–Muggianu model; Activity; Excess Gibbs energy; Ternary and binary *L*-parameters

1. Introduction

The search for a replacement to lead solder in the electronic industry has increased significantly during the last decade. According to the European Directive covering "Waste from Electrical and Electronic Equipment" (WEEE Directive from 2000) it was proposed to ban the use of Lead solders completely after January 2008. It is now widely agreed that there will be no single drop-in replacement for lead–tin solders and that the final choice of solder material will be application-dependent. Thus, a number of possible replacements are being investigated including binary, ternary and even quaternary alloy systems composed of Sn, Cu, Ag, In, Zn, Ni, Au, and Pd. Indium is included here due to its low melting point while palladium, gold, copper and nickel also represent possible substrates. From the list of elements, the Ag–In–Sn and Cu–In–Sn ternary alloy systems are regarded as two possible candidates for replacing lead–tin solder, Ag–In–Sn being of interest in the present work. The full thermodynamic description of an alloy system is possible if Gibbs energy of all phases present in equilibrium at given temperature is known.

All binary combinations of possible elements have been studied using different methods to obtain their activities and other thermodynamic quantities of mixing. Those data were further used to make a critical assessment of a particular binary system in the literature. As a result, a set of thermodynamic parameters is available to describe the phase equilibrium of binary systems. However, for ternary and quaternary systems, the greater number of solid phases makes the situation more complex and less experimental

* Corresponding author. Tel.: +36 1 2090555/1571; fax: +36 1 2090602.
E-mail address: bencze@chem.elte.hu (L. Bencze).

1387-3806/$ – see front matter © 2007 Elsevier B.V. All rights reserved.
doi:10.1016/j.ijms.2007.12.008

activity data and phase diagram information exist. In general, the interaction parameters are obtained from various experimental data including a phase diagram, chemical potential, thermodynamic activity, and enthalpy data either by trial and error or better still mathematically using CALPHAD methods [1–3].

In 2001 Miki et al. [4] were able to show that by using the Redlich–Kister–Muggianu (RKM) sub-regular solution model they could obtain the ternary interaction parameters from direct mass spectrometric measurements. However, Miki et al. [4], as a simplification, assumed only one kind of ternary L-parameter instead of the generally accepted three parameters. In addition, they determined the L-parameter and the thermodynamic data measuring only the Ag^+ to In^+ ion intensity ratio. Our aim was to elaborate the corresponding mathematical regression procedure for the Ag^+ to Sn^+ ion intensity ratio and to study the mathematical relationship between the two procedures based on both ion intensity ratios and to compare the data obtained by both procedures. In addition, we confirmed the reliability of the data using standard, model-free KEMS procedures as well. More recently, Schmidt and Tomiska [5] independently developed a similar mass spectrometric regression method not by using the RKM ternary L-parameters but by the so-called thermodynamic adoptive parameter series (TAP) for the description of the individual phases. Recently, we applied Miki et al. [4] method supplemented by us in Ref. [6] to the Cu–In–Sn system using only Cu^+ to Sn^+ ion intensity ratio to determine all the three ternary interaction parameters of the Cu–In–Sn liquid system. Excess enthalpy data on the Ag–In–Sn system are available in Refs. [7–9,10] whereas the excess Gibbs energies and activities are available only in Miki et al. article [4] so far.

2. Experimental

In this work a Nier type magnetic mass spectrometer was used in combination with a single Knudsen cell. The experimental technique is described in full elsewhere [11]. In a typical experiment the sample is heated in the cell to the desired temperature. Vapours, effusing through a small cell orifice, are admitted into the ionisation chamber of the ion source where they are ionised (30 eV) and detected and their abundances measured using an electron multiplier operated in the counting mode at −3.0 kV feed (for a detailed description of experimental setup, see Ref. [12]. In such an arrangement, above the condensed sample, the equilibrium vapour pressure (p_j) of the molecular species 'j', within the Knudsen cell, can be obtained using Eq. [1]

$$p_j = \frac{KT}{\sigma_j} \sum_k \frac{I_{jk}^+}{\eta_k \gamma_k} \tag{1}$$

where I_{jk}^+ is the intensity of ion k formed from the molecular species j, T is the absolute temperature of the Knudsen cell, K is the general sensitivity constant of the particular instrument, σ_j is the ionisation cross-section of molecular species j at the measured ionising electron energy, η_k is the isotope abundance of ion k and γ_k is the multiplier efficiency for ion k.

We can also obtain the variation of the vapour pressure ratio of the two given species with temperature by measuring the corresponding ion intensity ratio without explicit knowledge of the values of the parameters in Eq. (1). This important feature of KEMS, as a relative method, makes it an efficient technique for measuring the activities and thermodynamic quantities of binary systems [13]. Using relative KEMS methods it is not necessary to calculate the vapour pressures of the components, the activities can be obtained directly from the measured ion intensities.

2.1. Sample preparation and measuring procedure

Weighted amounts of metals obtained from Sigma–Aldrich (500 mg of total mass) were collected in a small alumina cup and placed in a vertical quartz tube into which a 7% hydrogen in argon mixture was fed during the melting procedure at 800 °C for several hours. The use of a reductive atmosphere during the melt was necessary to expel any trace of oxygen present in the metals either as a surface or bulk impurity. When using pure (99.99%) argon as protective gas high intensity of In_2O^+ ion appeared in the mass spectrum. $In_2O(g)$ is formed according to the following reaction below [14]:

$$In_2O_3(s) + 4In(l) = 3In_2O(g) \tag{2}$$

The high volatility of In_2O enhanced the loss of indium during its pressure determination (mass loss experiments) as will be described later. Nevertheless, it was impossible to avoid traces of the $In_2O^+(g)$ ion. In a typical experiment the sample was loaded in a cylindrical alumina cell (10 mm long, 10 mm in diameter) with a channel type orifice of 0.55 mm diameter. The cell was inserted into the Knudsen evaporator [7] and evacuated to high vacuum. The cell was then heated to 1200 °C at 20 °C/min. The abundance of In_2O^+ was monitored during the temperature rise. At 1200 °C the ion abundance rapidly falls off to below 500 counts/s. A typical mass loss (loss of mostly indium) during this heat treatment was less that 0.5 mg. Soon after reaching 1200 °C the intensities of the $^{107}Ag^+$, $^{115}In^+$ and $^{120}Sn^+$ ions were measured at every 10 °C down to 1000 °C.

2.2. Determination of thermodynamic quantities of mixing by conventional KEMS methods and a new method based on the Redlich–Kister–Muggianu sub-regular solution model

The excess Gibbs energy of ternary liquid mixtures, taking both binary and ternary interactions into account, can be described as random mixtures of components A, B and C by a sub regular-solution type model after Muggianu et al. [15] as (Eq. [3]):

$$G^{\mathrm{E}} = X_{\mathrm{A}}X_{\mathrm{B}}\sum_{i=0}^{n_{\mathrm{AB}}} L^{i}_{\mathrm{AB}}(X_{\mathrm{A}}-X_{\mathrm{B}})^{i} + X_{\mathrm{A}}X_{\mathrm{C}}\sum_{i=0}^{n_{\mathrm{AC}}} L^{i}_{\mathrm{AC}}(X_{\mathrm{A}}-X_{\mathrm{C}})^{i} + X_{\mathrm{B}}X_{\mathrm{C}}\sum_{i=0}^{n_{\mathrm{BC}}} L^{i}_{\mathrm{BC}}(X_{\mathrm{B}}-X_{\mathrm{C}})^{i} + X_{\mathrm{A}}X_{\mathrm{B}}X_{\mathrm{C}}[L^{0}_{\mathrm{ABC}}X_{\mathrm{A}} + L^{1}_{\mathrm{ABC}}X_{\mathrm{B}} + L^{2}_{\mathrm{ABC}}X_{\mathrm{C}}] \quad (3)$$

where X_{A}, X_{B} and X_{C} are the mole fractions, L's are the so-called binary and ternary interaction parameters. For a real system the notations A, B and C have to be replaced by the formulae of the real components (in our case elements) in alphabetic order, *i.e.*, *e.g.*, A = Cu, B = In and C = Sn. Whereas the number of binary L-parameters (n_{AB}, n_{AC} and n_{BC}) used in Eq. (3) depends on the best fit for the measured binary data the number of ternary L-parameters is strictly three. Nevertheless, in simplified cases only one ternary L_{ABC} is assumed (Miki et al.'s [4] assumption, $L^{0}_{\mathrm{ABC}} = L^{1}_{\mathrm{ABC}} = L^{2}_{\mathrm{ABC}} = L_{\mathrm{ABC}}$, see *e.g.*, Ref. [4]).In our work on Cu–In–Sn system [6] we have shown that the ternary L-parameters and the intercept C can be determined using Eq. [4] below:

$$Ysumma = -C + L^{0}_{\mathrm{CuInSn}}(2X_{\mathrm{Sn}} - X_{\mathrm{Cu}})X_{\mathrm{Cu}}X_{\mathrm{In}} + L^{1}_{\mathrm{CuInSn}}(X_{\mathrm{Sn}} - X_{\mathrm{Cu}})(X_{\mathrm{In}})^{2} + L^{2}_{\mathrm{CuInSn}}(X_{\mathrm{Sn}} - 2X_{\mathrm{Cu}})X_{\mathrm{Sn}}X_{\mathrm{In}} \quad (4)$$

where the intercept C is a constant including the standard Gibbs energies of evaporation of the pure elements (Cu and Sn) and the parameters described in Eq. (1). Furthermore,

$$Ysumma \equiv Y + YY \quad (5)$$

$$YY \equiv RT\ln\left(\frac{I_{\mathrm{Cu}}X_{\mathrm{Sn}}}{I_{\mathrm{Sn}}X_{\mathrm{Cu}}}\right) \quad (6)$$

$$Y \equiv -\{X_{\mathrm{In}}[L^{0}_{\mathrm{CuIn}} + L^{1}_{\mathrm{CuIn}}(X_{\mathrm{Cu}} - X_{\mathrm{In}}) + L^{2}_{\mathrm{CuIn}}(X_{\mathrm{Cu}} - X_{\mathrm{In}})^{2}] + X_{\mathrm{Cu}}X_{\mathrm{In}}[L^{1}_{\mathrm{CuIn}} + 2L^{2}_{\mathrm{CuIn}}(X_{\mathrm{Cu}} - X_{\mathrm{In}})] + (1 - X_{\mathrm{In}} - 2X_{\mathrm{Cu}})[L^{0}_{\mathrm{CuSn}} + L^{1}_{\mathrm{CuSn}}(2X_{\mathrm{Cu}} - 1 + X_{\mathrm{In}}) + L^{2}_{\mathrm{CuSn}}(2X_{\mathrm{Cu}} - 1 + X_{\mathrm{In}})^{2}] + X_{\mathrm{Cu}}(1 - X_{\mathrm{In}} - X_{\mathrm{Cu}})[2L^{1}_{\mathrm{CuSn}} + 4L^{2}_{\mathrm{CuSn}}(2X_{\mathrm{Cu}} - 1 + X_{\mathrm{In}})] - X_{\mathrm{In}}[L^{0}_{\mathrm{InSn}} + L^{1}_{\mathrm{InSn}}(3X_{\mathrm{In}} - 2 + 2X_{\mathrm{Cu}})]\} \quad (7)$$

where I denotes the mass spectrometric ion intensity and obviously $X_{\mathrm{Cu}} + X_{\mathrm{In}} + X_{\mathrm{Sn}} = 1$. The L-parameters in Eq. (7) are the binary L-parameters of the three boundary binary systems and taken from the literature if own measurements are not available.

For 'n' compositions of the ternary alloy Eq. [4] can be written as a set of linear equations, and, if $n > 4$ the solution of the parallel linear equations has to be replaced with a multiple regression problem:

$$\begin{bmatrix} 1 & ((2X_{\mathrm{Sn}} - X_{\mathrm{Cu}})X_{\mathrm{Cu}}X_{\mathrm{In}})_1 & ((X_{\mathrm{Sn}} - X_{\mathrm{Cu}})X^{2}_{\mathrm{In}})_1 & ((X_{\mathrm{Sn}} - 2X_{\mathrm{Cu}})X_{\mathrm{Sn}}X_{\mathrm{In}})_1 \\ 1 & ((2X_{\mathrm{Sn}} - X_{\mathrm{Cu}})X_{\mathrm{Cu}}X_{\mathrm{In}})_2 & ((X_{\mathrm{Sn}} - X_{\mathrm{Cu}})X^{2}_{\mathrm{In}})_2 & ((X_{\mathrm{Sn}} - 2X_{\mathrm{Cu}})X_{\mathrm{Sn}}X_{\mathrm{In}})_2 \\ . & . & . & . \\ 1 & ((2X_{\mathrm{Sn}} - X_{\mathrm{Cu}})X_{\mathrm{Cu}}X_{\mathrm{In}})_n & ((X_{\mathrm{Sn}} - X_{\mathrm{Cu}})X^{2}_{\mathrm{In}})_n & ((X_{\mathrm{Sn}} - 2X_{\mathrm{Cu}})X_{\mathrm{Sn}}X_{\mathrm{In}})_n \end{bmatrix} \begin{bmatrix} -C \\ L^{0}_{\mathrm{CuInSn}} \\ L^{1}_{\mathrm{CuInSn}} \\ L^{2}_{\mathrm{CuInSn}} \end{bmatrix} = \begin{bmatrix} Ysumma_1 \\ Ysumma_2 \\ . \\ Ysumma_n \end{bmatrix} \quad (8)$$

where 'n' is the number of the measured compositions.

Changing from Cu–In–Sn system to Ag–In–Sn system, but still measuring the ion intensity of Sn^{+} beside that of Ag^{+} (like Cu^{+} in Cu–In–Sn), YY includes $I_{Ag^{+}}$ ion intensity instead of $I_{Cu^{+}}$. The construction of Y can also change if more (or less) binary L-parameters are used in the description of the corresponding boundary binary systems of Ag–In–Sn relative to that of Cu–In–Sn:

$$Ysumma_{\mathrm{AgInSn}(Ag^{+}/Sn^{+})} = -C_{\mathrm{AgInSn}(Ag^{+}/Sn^{+})} + L^{0}_{\mathrm{AgInSn}}(2X_{\mathrm{Sn}} - X_{\mathrm{Ag}})X_{\mathrm{Ag}}X_{\mathrm{In}} + L^{1}_{\mathrm{AgInSn}}(X_{\mathrm{Sn}} - X_{\mathrm{Ag}})(X_{\mathrm{In}})^{2} + L^{2}_{\mathrm{AgInSn}}(X_{\mathrm{Sn}} - 2X_{\mathrm{Ag}})X_{\mathrm{Sn}}X_{\mathrm{In}} \quad (9)$$

$$Ysumma_{\mathrm{AgInSn}(Ag^{+}/Sn^{+})} \equiv Y_{\mathrm{AgInSn}(Ag^{+}/Sn^{+})} + YY_{\mathrm{AgInSn}(Ag^{+}/Sn^{+})} \quad (10)$$

$$YY_{\mathrm{AgInSn}(Ag^{+}/Sn^{+})} \equiv RT\ln\left(\frac{I_{\mathrm{Ag}}X_{\mathrm{Sn}}}{I_{\mathrm{Sn}}X_{\mathrm{Ag}}}\right) \quad (11)$$

$$Y_{\mathrm{AgInSn}(Ag^{+}/Sn^{+})} \equiv -\{X_{\mathrm{In}}[L^{0}_{\mathrm{AgIn}} + L^{1}_{\mathrm{AgIn}}(X_{\mathrm{Ag}} - X_{\mathrm{In}}) + L^{2}_{\mathrm{AgIn}}(X_{\mathrm{Ag}} - X_{\mathrm{In}})^{2} + L^{3}_{\mathrm{AgIn}}(X_{\mathrm{Ag}} - X_{\mathrm{In}})^{3}] + X_{\mathrm{Ag}}X_{\mathrm{In}}[L^{1}_{\mathrm{AgIn}} + 2L^{2}_{\mathrm{AgIn}}(X_{\mathrm{Ag}} - X_{\mathrm{In}}) + 3L^{3}_{\mathrm{AgIn}}(X_{\mathrm{Ag}} - X_{\mathrm{In}})^{2}] + (1 - X_{\mathrm{In}} - 2X_{\mathrm{Ag}})$$

$$\times [L^0_{\mathrm{AgSn}} + L^1_{\mathrm{AgSn}}(2X_{\mathrm{Ag}} - 1 + X_{\mathrm{In}}) + L^2_{\mathrm{AgSn}}(2X_{\mathrm{Ag}} - 1 + X_{\mathrm{In}})^2 + L^3_{\mathrm{AgSn}}(2X_{\mathrm{Ag}} - 1 + X_{\mathrm{In}})^3]$$
$$+ X_{\mathrm{Ag}}(1 - X_{\mathrm{In}} - X_{\mathrm{Ag}})[2L^1_{\mathrm{AgSn}} + 4L^2_{\mathrm{AgSn}}(2X_{\mathrm{Ag}} - 1 + X_{\mathrm{In}}) + 6L^3_{\mathrm{AgSn}}(2X_{\mathrm{Ag}} - 1 + X_{\mathrm{In}})^2]$$
$$- X_{\mathrm{In}}[L^0_{\mathrm{InSn}} + L^1_{\mathrm{InSn}}(3X_{\mathrm{In}} - 2 + 2X_{\mathrm{Ag}})]\} \quad (12a)$$

since L^3_{AgIn} and L^3_{AgSn} are not zero unlike L^3_{CuIn} and L^3_{CuSn}. As can be seen, L^2_{InSn} and L^3_{InSn} are considered zero like in the case of the Cu–In–Sn system if the same In–Sn binary database (Miki et al.'s own database [4]) is used for both ternary systems. Nevertheless, we have used the same binary databases [16–18] as Miki et al.'s [4] for all the three boundary binary systems of Ag–In–Sn. As a particular case, Eq. (7) can be obtained from Eq. (12a) if Ag is replaced with Cu and the replacements $L^3_{\mathrm{CuIn}} = 0$ and $L^3_{\mathrm{CuSn}} = 0$ are also performed.

By doing some replacements with the mole fractions and distributing the five-term-equation to a six-term-one for easier comparison, Eq. (12a) changes to Eq. (12b) as follows:

$$Y_{\mathrm{AgInSn(Ag^+/Sn^+)}} \equiv -\{X_{\mathrm{In}}[L^0_{\mathrm{AgIn}} + L^1_{\mathrm{AgIn}}(X_{\mathrm{Ag}} - X_{\mathrm{In}}) + L^2_{\mathrm{AgIn}}(X_{\mathrm{Ag}} - X_{\mathrm{In}})^2 + L^3_{\mathrm{AgIn}}(X_{\mathrm{Ag}} - X_{\mathrm{In}})^3]$$
$$+ X_{\mathrm{Ag}}X_{\mathrm{In}}[L^1_{\mathrm{AgIn}} + 2L^2_{\mathrm{AgIn}}(X_{\mathrm{Ag}} - X_{\mathrm{In}}) + 3L^3_{\mathrm{AgIn}}(X_{\mathrm{Ag}} - X_{\mathrm{In}})^2]$$
$$+ X_{\mathrm{Sn}}[L^0_{\mathrm{AgSn}} + L^1_{\mathrm{AgSn}}(X_{\mathrm{Ag}} - X_{\mathrm{Sn}}) + L^2_{\mathrm{AgSn}}(X_{\mathrm{Ag}} - X_{\mathrm{Sn}})^2 + L^3_{\mathrm{AgSn}}(X_{\mathrm{Ag}} - X_{\mathrm{Sn}})^3]$$
$$- X_{\mathrm{Ag}}[L^0_{\mathrm{AgSn}} + L^1_{\mathrm{AgSn}}(X_{\mathrm{Ag}} - X_{\mathrm{Sn}}) + L^2_{\mathrm{AgSn}}(X_{\mathrm{Ag}} - X_{\mathrm{Sn}})^2 + L^3_{\mathrm{AgSn}}(X_{\mathrm{Ag}} - X_{\mathrm{Sn}})^3]$$
$$+ X_{\mathrm{Ag}}X_{\mathrm{Sn}}[2L^1_{\mathrm{AgSn}} + 4L^2_{\mathrm{AgSn}}(X_{\mathrm{Ag}} - X_{\mathrm{Sn}}) + 6L^3_{\mathrm{AgSn}}(X_{\mathrm{Ag}} - X_{\mathrm{Sn}})^2] - X_{\mathrm{In}}[L^0_{\mathrm{InSn}} + L^1_{\mathrm{InSn}}(X_{\mathrm{In}} - 2X_{\mathrm{Sn}})]\} \quad (12b)$$

The thermodynamic properties of mixing of ternary liquid alloys like *e.g.*, Ag–In–Sn can be obtained by KEMS from more than one kind of ion intensity ratio. In the former investigation of Ag–In–Sn by Miki et al. [4] they used the Ag^+ to In^+ ion intensity ratio, whereas in our investigation of the Cu–In–Sn system [6] we used the Cu^+ to Sn^+ ion intensity ratio to determine mixing properties. In this paper we have elaborated the mathematical regression techniques for the determination of the ternary L's from both Ag^+ to In^+ and Ag^+ to Sn^+ ion intensity ratios for the first time. In addition, we have analysed the mathematical relationship between the two procedures and compared the data obtained by both. In Ref. [4] Miki et al. used a simplified model, assuming only one kind of ternary L_{AgInSn} instead of the generally used three L's (see Eq. [3]) and they determined L_{AgInSn} from Ag^+ to In^+ ion intensity ratio only.

In the case when Ag^+ and In^+, rather than Ag^+ and Sn^+ ion intensities are measured the three ternary L-parameters should be determined using Eq. (13):

$$Ysumma_{\mathrm{AgInSn(Ag^+/In^+)}} = -C_{\mathrm{AgInSn(Ag^+/In^+)}} + L^0_{\mathrm{AgInSn}}(2X_{\mathrm{In}} - X_{\mathrm{Ag}})X_{\mathrm{Ag}}X_{\mathrm{Sn}} + L^1_{\mathrm{AgInSn}}(X_{\mathrm{In}} - 2X_{\mathrm{Ag}})X_{\mathrm{Sn}}X_{\mathrm{In}}$$
$$+ L^2_{\mathrm{AgInSn}}(X_{\mathrm{In}} - X_{\mathrm{Ag}})(X_{\mathrm{Sn}})^2 \quad (13)$$

where $Ysumma_{\mathrm{AgInSn(Ag^+/In^+)}}$, $YY_{\mathrm{AgInSn(Ag^+/In^+)}}$ and $Y_{\mathrm{AgInSn(Ag^+/In^+)}}$ can be determined using Eqs. (14)–(16) below:

$$Ysumma_{\mathrm{AgInSn(Ag^+/In^+)}} \equiv Y_{\mathrm{AgInSn(Ag^+/In^+)}} + YY_{\mathrm{AgInSn(Ag^+/In^+)}} \quad (14)$$

$$YY_{\mathrm{AgInSn(Ag^+/In^+)}} \equiv RT \ln\left(\frac{I_{\mathrm{Ag}}X_{\mathrm{In}}}{I_{\mathrm{In}}X_{\mathrm{Ag}}}\right) \quad (15)$$

$$Y_{\mathrm{AgInSn(Ag^+/In^+)}} \equiv -\{X_{\mathrm{In}}[L^0_{\mathrm{AgIn}} + L^1_{\mathrm{AgIn}}(X_{\mathrm{Ag}} - X_{\mathrm{In}}) + L^2_{\mathrm{AgIn}}(X_{\mathrm{Ag}} - X_{\mathrm{In}})^2 + L^3_{\mathrm{AgIn}}(X_{\mathrm{Ag}} - X_{\mathrm{In}})^3]$$
$$+ X_{\mathrm{Ag}}X_{\mathrm{Sn}}[L^1_{\mathrm{AgSn}} + 2L^2_{\mathrm{AgSn}}(X_{\mathrm{Ag}} - X_{\mathrm{Sn}}) + 3L^3_{\mathrm{AgSn}}(X_{\mathrm{Ag}} - X_{\mathrm{Sn}})^2]$$
$$+ X_{\mathrm{Sn}}[L^0_{\mathrm{AgSn}} + L^1_{\mathrm{AgSn}}(X_{\mathrm{Ag}} - X_{\mathrm{Sn}}) + L^2_{\mathrm{AgSn}}(X_{\mathrm{Ag}} - X_{\mathrm{Sn}})^2 + L^3_{\mathrm{AgSn}}(X_{\mathrm{Ag}} - X_{\mathrm{Sn}})^3]$$
$$- X_{\mathrm{Ag}}[L^0_{\mathrm{AgIn}} + L^1_{\mathrm{AgIn}}(X_{\mathrm{Ag}} - X_{\mathrm{In}}) + L^2_{\mathrm{AgIn}}(X_{\mathrm{Ag}} - X_{\mathrm{In}})^2 + L^3_{\mathrm{AgIn}}(X_{\mathrm{Ag}} - X_{\mathrm{In}})^3]$$
$$+ X_{\mathrm{Ag}}X_{\mathrm{In}}[2L^1_{\mathrm{AgIn}} + 4L^2_{\mathrm{AgIn}}(X_{\mathrm{Ag}} - X_{\mathrm{In}}) + 6L^3_{\mathrm{AgIn}}(X_{\mathrm{Ag}} - X_{\mathrm{In}})^2] - X_{\mathrm{Sn}}[L^0_{\mathrm{InSn}} + L^1_{\mathrm{InSn}}(2X_{\mathrm{In}} - X_{\mathrm{Sn}})]\} \quad (16)$$

Comparing Eq. (16) to Eq. (12b) certain construction relations become apparent. Eq. (16) can be obtained from Eq. (12b) by replacing In with Sn and Sn with In, except that is for the last, sixth term, where, in addition, a sign change is required in front of the mole

fractions behind L^1_{InSn}. A relationship also exists between Eqs. (9) and (13): beside the exchange of subscripts Sn and In in the mole fractions the multipliers of L^1_{AgInSn} and L^2_{AgInSn} are also exchanged.

It can be noticed that the ternary L^0_{AgInSn}, L^1_{AgInSn} and L^2_{AgInSn} parameters can be obtained from both Eqs. (9) and (13) by multiple regression on different functions. This is the advantage of KEMS, *i.e.*, the whole mass spectrum can be used for the determination of ternary L's. Similarly to Eq. (8) the regression matrix equation based on Eqs. (9) and (13) can be expressed by Eqs. (17) and (18) as follows:

$$\begin{bmatrix} 1 & ((2X_{Sn}-X_{Ag})X_{Ag}X_{In})_1 & ((X_{Sn}-X_{Ag})X_{In}^2)_1 & ((X_{Sn}-2X_{Ag})X_{Sn}X_{In})_1 \\ 1 & ((2X_{Sn}-X_{Ag})X_{Ag}X_{In})_2 & ((X_{Sn}-X_{Ag})X_{In}^2)_2 & ((X_{Sn}-2X_{Ag})X_{Sn}X_{In})_2 \\ . & . & . & . \\ 1 & ((2X_{Sn}-X_{Ag})X_{Ag}X_{In})_n & ((X_{Sn}-X_{Ag})X_{In}^2)_n & ((X_{Sn}-2X_{Ag})X_{Sn}X_{In})_n \end{bmatrix} \begin{bmatrix} -C \\ L^0_{AgInSn} \\ L^1_{AgInSn} \\ L^2_{AgInSn} \end{bmatrix} = \begin{bmatrix} Ysumma_{(Ag^+/Sn^+)_1} \\ Ysumma_{(Ag^+/Sn^+)_2} \\ . \\ Ysumma_{(Ag^+/Sn^+)_n} \end{bmatrix} \tag{17}$$

$$\begin{bmatrix} 1 & ((2X_{In}-X_{Ag})X_{Ag}X_{Sn})_1 & ((X_{In}-2X_{Ag})X_{In}X_{Sn})_1 & ((X_{In}-X_{Ag})X_{Sn}^2)_1 \\ 1 & ((2X_{In}-X_{Ag})X_{Ag}X_{Sn})_2 & ((X_{In}-2X_{Ag})X_{In}X_{Sn})_2 & ((X_{In}-X_{Ag})X_{Sn}^2)_2 \\ . & . & . & . \\ 1 & ((2X_{In}-X_{Ag})X_{Ag}X_{Sn})_n & ((X_{In}-2X_{Ag})X_{In}X_{Sn})_n & ((X_{In}-X_{Ag})X_{Sn}^2)_n \end{bmatrix} \begin{bmatrix} -C \\ L^0_{AgInSn} \\ L^1_{AgInSn} \\ L^2_{AgInSn} \end{bmatrix} = \begin{bmatrix} Ysumma_{(Ag^+/In^+)_1} \\ Ysumma_{(Ag^+/In^+)_2} \\ . \\ Ysumma_{(Ag^+/In^+)_n} \end{bmatrix} \tag{18}$$

Using Eq. (3) the excess Gibbs energy can be obtained, and from this, the excess chemical potentials, the activity coefficients and the activities can be determined using the following well-known relationships (19)–(22):

$$a_i = X_i\gamma_i = X_i \exp\left(\frac{\mu_i^E}{RT}\right) \tag{19}$$

$$\mu_{Ag}^E = G^E - X_{In}\left(\frac{\partial G^E}{\partial X_{In}}\right)_{X_{Ag}} + (1-X_{Ag})\left(\frac{\partial G^E}{\partial X_{Ag}}\right)_{X_{In}} \tag{20}$$

$$\mu_{Sn}^E = G^E - X_{Ag}\left(\frac{\partial G^E}{\partial X_{Ag}}\right)_{X_{In}} - X_{In}\left(\frac{\partial G^E}{\partial X_{In}}\right)_{X_{Ag}} \tag{21}$$

$$\mu_{In}^E = G^E - X_{Ag}\left(\frac{\partial G^E}{\partial X_{Ag}}\right)_{X_{Sn}} - X_{Sn}\left(\frac{\partial G^E}{\partial X_{Sn}}\right)_{X_{Ag}} \tag{22}$$

where i denotes any of the components (Ag, In or Sn).

In addition, it is also possible to obtain from the temperature dependence of these quantities the partial molar and integral molar excess enthalpies and entropies.

Another type of KEMS experiments, involving the determination of activities, were performed using the conventional Knudsen effusion isothermal evaporation method (IEM) [11]. In the present case the method involved the measurement of mass loss rate of the alloy sample relative to the mass loss rate of the pure metal component at an equivalent temperature during an isothermal evaporation from the Knudsen cell. We performed such measurements at 900 °C. Since the volatility of indium is much higher (with orders of magnitude) than that of the other components this method was mainly used for the determination of activity of indium, as can be seen in Eq. (23):

$$a_{In} = \frac{(p_{In})_{sample}}{(p_{In})_{pure\ In}} = \frac{(dm/dt)_{sample}}{(dm/dt)_{pure\ In}} \approx \frac{(\Delta m/\Delta t)_{sample}}{(\Delta m/\Delta t)_{pure\ In}} \tag{23}$$

where Δm and Δt represent the mass loss and the duration of evaporation, respectively. This simple relation implies that we can determine the activity with a high accuracy. The only small systematic error being due to the enhanced evaporation of indium via loss of $In_2O(g)$ from the thin oxide surface layer and slight change in composition during incongruent evaporation (distillation). The equality between the left and right hand sides of Eq. (23) is valid in the only case if no composition shift (distillation) occurs. A typical mass loss from starting 1000 mg of sample was only 2–4 mg. Therefore, practically no composition correction was needed. It was also assumed, that at 900 °C contributions of Cu and Sn to the total mass loss is negligible and does not affect the final result. To determine the activities of the other two components not only the total mass loss but also the mass spectrum is needed. This method,

that is also called an isothermal evaporation method but is in reality a mass spectrometry (MS) method, is based on the well-known Hertz–Knudsen equation, as follows:

$$p_{Ag} = \frac{KT}{\sigma_{Ag}\eta_{Ag^+}\gamma_{Ag^+}} I_{Ag^+} \quad \text{and} \quad p_{In} = \frac{KT}{\sigma_{In}\eta_{In^+}\gamma_{In^+}} I_{In^+} \quad \text{and} \quad p_{Sn} = \frac{KT}{\sigma_{Sn}\eta_{Sn^+}\gamma_{Sn^+}} I_{Sn^+}$$

where

$$K = \sqrt{\frac{2\pi R}{T}} \frac{\Delta m}{W_B A\, \Delta t} \left(\frac{I_{Ag^+}}{\sigma_{Ag}\eta_{Ag^+}\gamma_{Ag^+}} \sqrt{M_{Ag}} + \frac{I_{In^+}}{\sigma_{In}\eta_{In^+}\gamma_{In^+}} \sqrt{M_{In}} + \frac{I_{Sn^+}}{\sigma_{Sn}\eta_{Sn^+}\gamma_{Sn^+}} \sqrt{M_{Sn}} \right)^{-1} \tag{24}$$

where K is the sensitivity constant of the mass spectrometer, M is the molar mass of the effusing gaseous molecules, A is the area of the orifice of the Knudsen cell, W_B is the Clausing factor of the orifice and R is the universal gas constant.

Such experiments on Ag–In–Sn were carried out by us at 1050 and 1100 °C. The IEM was used only to compare the experimental data to the values yielded by the RKM model since the mass loss measurements are time consuming and the data obtained from a single evaporation experiment are available only for that particular temperature of the evaporation experiment.

The third method, that is also a conventional KEMS technique, used for the determination of activities of Ag, In and Sn was the so-called Gibbs–Duhem ion intensity ratio (GD-IIR) method, introduced by Belton and Fruehan for binary and ternary systems [19]. This method was also used for comparison purposes since the calculations were made only on the measured compositions (without interpolation). A study by Bencze et al., applying this method to a ternary solid Al–Fe–Ni system can be found in Ref. [20]. The activity coefficients of the components in the Ag–In–Sn system using GD-IIR method, can be expressed by Eqs. (25)–(27) as follows:

$$\ln\gamma_{In}(X) = \ln\gamma_{In}(X_{ref}) - \int_{X_{ref}}^{X} X_{Ag}\, d\ln\left(\frac{I^+_{Ag}X_{In}}{I^+_{In}X_{Ag}}\right) - \int_{X_{ref}}^{X} X_{Sn}\, d\ln\left(\frac{I^+_{Sn}X_{In}}{I^+_{In}X_{Sn}}\right) \tag{25}$$

$$\ln\gamma_{Sn}(X) = \ln\gamma_{Sn}(X_{ref}) - \int_{X_{ref}}^{X} X_{In}\, d\ln\left(\frac{I^+_{In}X_{Sn}}{I^+_{Sn}X_{In}}\right) - \int_{X_{ref}}^{X} X_{Ag}\, d\ln\left(\frac{I^+_{Ag}X_{Sn}}{I^+_{Sn}X_{Ag}}\right) \tag{26}$$

$$\ln\gamma_{Ag}(X) = \ln\gamma_{Ag}(X_{ref}) - \int_{X_{ref}}^{X} X_{In}\, d\ln\left(\frac{I^+_{In}X_{Ag}}{I^+_{Ag}X_{In}}\right) - \int_{X_{ref}}^{X} X_{Sn}\, d\ln\left(\frac{I^+_{Sn}X_{Ag}}{I^+_{Ag}X_{Sn}}\right) \tag{27}$$

3. Results and discussion

The experimental compositions of Ag–In–Sn alloys are shown in Fig. 1. Nevertheless, since not all compositions have been measured under the same ion source/detector conditions these compositions have to be treated in two separate datasets including three runs for the RKM regression.

As usual in KEMS investigations made over a medium temperature range (100–200 K), the logarithm of the measured ion intensity ratio *versus* reciprocal of temperature at a fixed composition is a linear function showing no temperature dependence of the enthalpy change of evaporation (or sublimation). The A and B parameters of both $\ln(I^+_{Ag}/I^+_{In}) = A_{AgIn} + B_{AgIn}/T$ and $\ln(I^+_{Ag}/I^+_{Sn}) = A_{AgSn} + B_{AgSn}/T$ can be seen in Table 1. The minus slope (B) multiplied with the universal gas constant (R) represents the difference of the enthalpy changes of evaporation of the two components. The measured values of $\ln(I^+_{Ag}/I^+_{In})$ *versus* $1/T$ and that of $\ln(I^+_{Ag}/I^+_{Sn})$ *versus* $1/T$ for some selected measured compositions are plotted in Fig. 2.

The binary L-parameters necessary for performing the RKM model calculations were taken from Refs. [16–18]; the same parameters were also used by Miki et al. [4]. Table 2 gives a comparison of the binary L-data taken from Refs. [16–18] and from the COST 531 database [21]. The original sources of the liquid binary L-data of Ag–In, Ag–Sn and In–Sn systems in Ref. [21] can also be found in Refs. [22–24], respectively. A comparison of the binary G^E data between these two literature sources can be seen in Fig. 3. We have already discussed in Ref. [6] that the literature sources of In–Sn binary L-parameters are very different and, as a result, are the corresponding excess Gibbs energy *versus* composition functions. However, this is not problematic since In–Sn makes only a minor contribution to the total G^E of the ternary alloy. However, this is not the case for Ag–In and Ag–Sn systems concerning the ternary alloy, and, the differences observed in the thermodynamic data of the ternary alloy needs further discussion.

Taking the measured ion intensity ratio data *YY*, whereas using the binary L's from Refs. [16–18] Y can be calculated. In the next step *Ysumma* are calculated in order to fit the data to the RKM model according to Eqs. (9)–(12a) and (13)–(16). Eqs. (9) and (13) reveal *Ysumma versus* the three independent variables to be four-dimensional functions. Beside the correlation coefficient of the multi-linear regression, in order to present the correlation of the data in a graphical form, the appropriate two-dimensional functions could be plotted. Fig. 4 shows a plot of the calculated *Ysumma*, *i.e.*, *Ysummacalc*, is plotted against *Ysumma*. *Ysummacalc* is calculated by multiplying the ternary L-parameters, obtained from the multi-linear regression, with the corresponding three independent variables including the mole fractions.

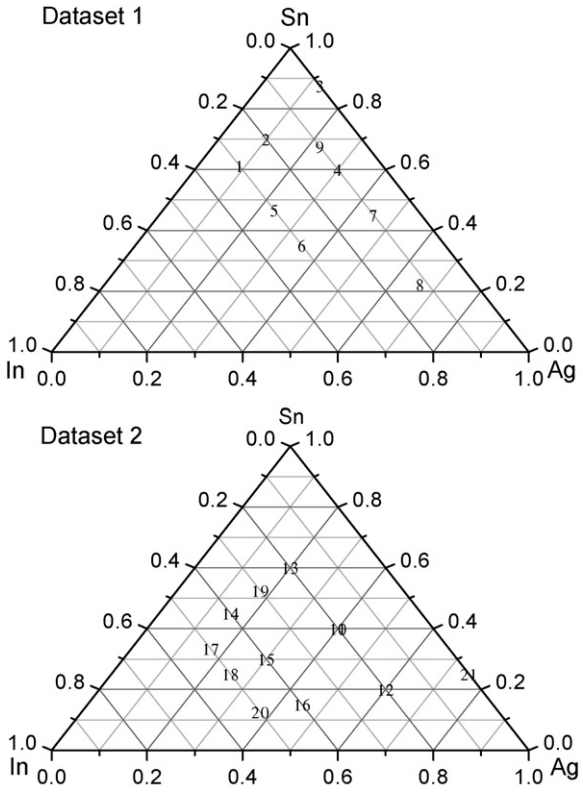

Fig. 1. Composition of the samples measured.

Table 1
The parameters of $\ln(I^+_{Ag}X_{Sn}/I^+_{Sn}X_{Ag}) = A_{AgSn} + (B_{AgSn}/T)$ and $\ln(I^+_{Ag}X_{In}/I^+_{In}X_{Ag}) = A_{AgIn} + (B_{AgIn}/T)$ equations for all the measured compositions

Sample	Composition			$\ln\left(\frac{I^+_{Ag}X_{Sn}}{I^+_{Sn}X_{Ag}}\right) = A_{AgSn} + \left(\frac{B_{AgSn}}{T}\right)$		$\ln\left(\frac{I^+_{Ag}X_{In}}{I^+_{In}X_{Ag}}\right) = A_{AgIn} + \left(\frac{B_{AgIn}}{T}\right)$	
	X_{Ag}	X_{Sn}	X_{In}	A_{AgSn}	B_{AgSn}	A_{AgIn}	B_{AgIn}
				Dataset 1 (Run 1)		Dataset 1 (Run 2)	
1	0.088	0.612	0.300	0.3331[a]	3300.1[a]	–	–
2	0.100	0.700	0.200	0.4041[a]	3230.1[a]	–	–
3	0.125	0.875	0	0.5657	3510.1	–	–
4	0.300	0.600	0.100	0.4741[a]	3283.9[a]	−0.9127[a]	−3741.4[a]
5	0.233	0.467	0.300	1.2503	2416.0	−0.5876[a]	−4249.1[a]
6	0.350	0.350	0.300	1.0595[a]	2486.7[a]	−0.1344[a]	−4672.2[a]
7	0.450	0.450	0.100	0.8924[a]	2861.7[a]	−0.5064[a]	−4052.8[a]
8	0.662	0.221	0.117	1.6976[a]	2534.2[a]	−0.1093[a]	−3767.3[a]
9	0.225	0.675	0.100	0.2869[a]	3530.2[a]	−0.7356[a]	−3917.5[a]
				Dataset 2 (Run 3)		–	
10	0.400	0.400	0.200	1.5695[a]	1765.8[a]	–	–
11	0.400	0.400	0.200	1.4251	1976.6	–	–
12	0.600	0.200	0.200	2.4005[a]	1208.2[a]	–	–
13	0.200	0.600	0.200	0.6746[a]	2864.0[a]	–	–
14	0.150	0.450	0.400	1.4092[a]	1937.1[a]	–	–
15	0.300	0.300	0.400	1.2979[a]	1948.4[a]	–	–
16	0.450	0.150	0.400	1.5205[a]	1703.8[a]	–	–
17	0.167	0.333	0.500	1.4207[a]	1673.3[a]	–	–
18	0.250	0.250	0.500	1.1724	1893.8	–	–
19	0.175	0.525	0.300	−0.2876	4280.9	–	–
20	0.375	0.125	0.500	1.5552	1286.7	–	–

[a] Used for multiple RKM regression.

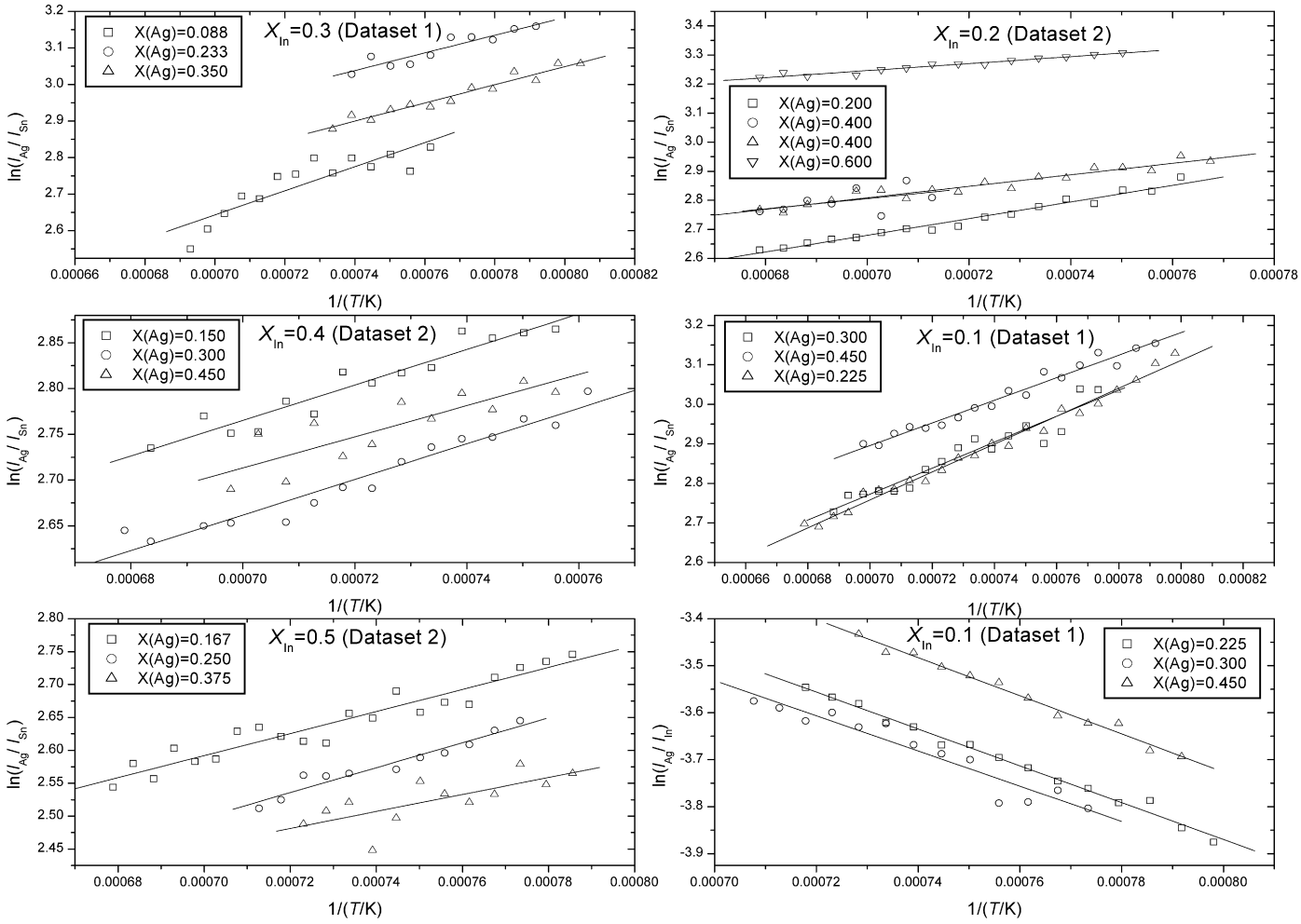

Fig. 2. The measured values of $\ln(I^+_{Ag}/I^+_{In})$ *vs.* $1/T$ and that of $\ln(I^+_{Ag}/I^+_{Sn})$ *vs.* $1/T$ for the measured compositions.

Table 3 gives the obtained ternary L-parameters at the five selected temperatures. The temperature dependence of the obtained ternary L's was expressed in the general form $A + BT + CT\ln(T)$. In addition to L^0_{AgInSn}, L^1_{AgInSn} and L^2_{AgInSn} determined from our own measurements, as a comparison, we also determined the same quantities from the measured raw I^+_{Ag}/I^+_{In} data of Miki et al. [4] since they originally applied a simplified Redlich–Kister–Muggianu model, resulting in only one kind of ternary L. Although, as can be seen from Table 3, both the absolute values of all kinds of ternary L's and the parameters of their temperature dependence

Table 2
Binary L-databases suggested by COST 531 datbase [21] and obtained from Refs. [16–18]

	Databases in Refs. [16–18] used also by Miki et al. [4]				COST 531 database [21]			
	A	B	C	L at 1273 K	A	B	C	L at 1273 K
L^0_{AgIn}	−16506	−3.6157	0	-2.111×10^4	−14403.297	−8.716	0	-2.481×10^4
L^1_{AgIn}	−11812	1.9389	0	-9.344×10^3	−15551.028	−2.664	0	-1.894×10^4
L^2_{AgIn}	0	0	0	0	−710.629	−5.293	0	-7.449×10^3
L^3_{AgIn}	0	0	0	0	3955.27	0	0	3.955×10^3
L^0_{AgSn}	−6386.2	−5.6668	0	-1.360×10^4	−5146.7	−5.0103	0	-1.152×10^4
L^1_{AgSn}	−14689	3.3398	0	-1.044×10^4	−15799.3	3.3208	0	-1.157×10^4
L^2_{AgSn}	−5339.3	1.058	0	-3.992×10^3	−6687.5	0	0	-6.688×10^3
L^3_{AgSn}	1943.6	−1.0001	0	670.473	0	0	0	0
L^0_{InSn}	−711	−1.6934	0	-2.867×10^3	−828.54	0.76018	−0.0526	−339.775
L^1_{InSn}	−64	−1.3592	0	-1.794×10^3	−115.59	−1.39997	0	-1.898×10^3
L^2_{InSn}	0	0	0	0	0	0	0	0
L^3_{InSn}	0	0	0	0	0	0	0	0

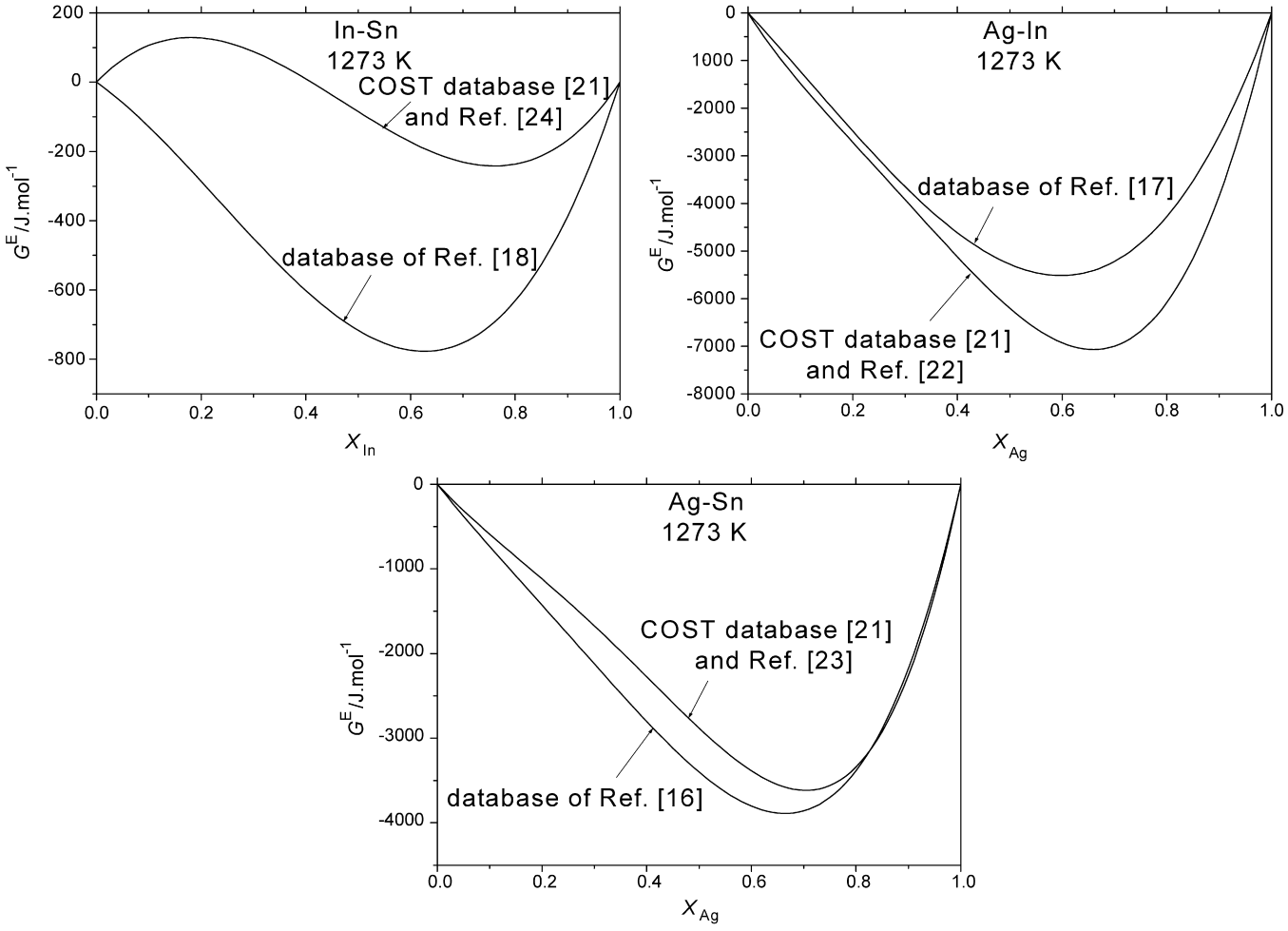

Fig. 3. Excess Gibbs energies of the three boundary binary systems obtained from Refs. [16–18] and from the COST database.

(*A*, *B* and *C*) do not agree for our own three runs (Runs 1–3) and Miki's measurement, the obtained G^E and the activities agree surprisingly well (Fig. 5).

Whereas the agreement between the values of our own two C_{AgSn} values is excellent, the agreement among the three parallel values of L^0_{AgInSn} is poor and, among the values of L^1_{AgInSn} is even worse. This poor reproducibility of our own ternary *L*'s must arise from the measurement uncertainties, *i.e.*, from the statistical error due to the relatively low number of compositions in each run. The deviation from the ternary *L*-data of Miki et al. [4] can be attributed to instrumentation and to statistical error, since the same input binary *L*'s were used in both cases. This latter deviation is not surprising since similar a relatively large deviation is observed in the values of binary *L*'s from different literature sources as can be seen in Table 2 concerning our boundary binary systems as well. Nevertheless, we expected a lower statistical error in our own parallel experiments. In spite of the weak reproducibility of the ternary *L*'s there must be a compensation effect on them, *i.e.*, there must be a correlation among L^0_{AgInSn}, L^1_{AgInSn} and L^2_{AgInSn} from one run to another resulting in surprisingly very small differences in the values of G^E at 1273 K (Fig. 5). These differences are small over the complete measured temperature range (1273–1473 K) as well. Similarly, negligible differences can be seen among the different runs concerning the values of the corresponding activities (Fig. 6). In addition, a very low deviation can be observed from Miki et al.'s [4] G^E and activity data as well. In spite of the good reproducibility of activities and G^E but due to the poor reproducibility of ternary *L*'s, for the phase diagram calculations, we recommend using only the ternary *L* data obtained from Miki et al.'s [4] raw Ag^+/In^+ intensity ratio data since more compositions are involved in Authors work. The recommended ternary *L*'s, evaluated by us, are as follows:

$$L^0_{AgInSn} = (-70,027 \pm 0) + (89 \pm 0)T \tag{28}$$

$$L^1_{AgInSn} = (145,900 \pm 1400) - (86.0 \pm 8.2)T + (0.77 \pm 0.99)T\ln(T) \tag{29}$$

$$L^2_{AgInSn} = (-122,900 \pm 1100) - (72.7 \pm 6.4)T - (0.95 \pm 0.78)T\ln(T) \tag{30}$$

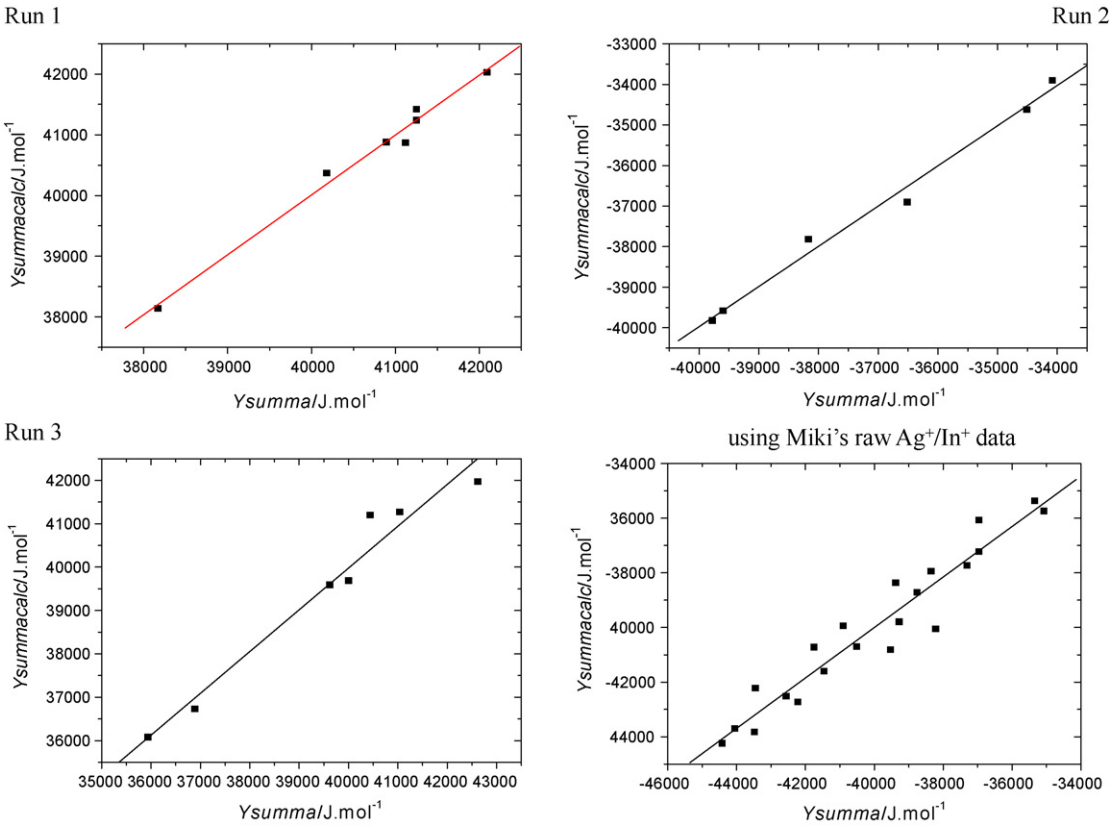

Fig. 4. *Ysummacalc* as a function of *Ysumma* obtained from all of our Runs and from Miki et al.'s [4] raw data at 1273 K.

Table 3
Ternary *L*-parameters obtained by the multi-linear regression at five selected temperatures using the binary *L*-databases from Refs. [16–18] and using the ion intensity ratios measured by KEMS (I^+_{Ag}/I^+_{Sn} and I^+_{Ag}/I^+_{In} ion intensity ratios in this work and the I^+_{Ag}/I^+_{In} ion intensity ratio of Miki et al. [4])

T (K)	Obtained from the I^+_{Ag}/I^+_{Sn} ratios of this work (Dataset 1 (Run 1))				Obtained from the I^+_{Ag}/I^+_{In} ratios of this work (Dataset 1 (Run 2))			
	$-C_{AgSn}$ (intercept)	L^0	L^1	L^2	$-C_{AgIn}$ (intercept)	L^0	L^1	L^2
1273	39310	56700	14940	3967	−36150	54000	1827	8923
1323	39740	52060	20320	2154	−36380	53990	−2483	10460
1373	40180	47430	25700	340.8	−36620	53980	−6794	11990
1423	40610	42790	31070	−1472	−36860	53970	−11100	13520
1473	41040	38150	36450	−3285	−37100	53960	−15410	15050
	$-C_{AgSn} = 27{,}230 + 15.01T - 0.772T\ln(T)$, $L^0 = 173{,}700 - 86.39T - 0.772T\ln(T)$, $L^1 = -123{,}500 + 114.078T - 0.795T\ln(T)$, $L^2 = 50{,}170 - 36.514T + 0.031T\ln(T)$, $\frac{\sigma_{Sn}\eta_{Sn}}{\sigma_{Ag}\eta_{Ag}} = 1.13 \pm 0.01 \Rightarrow \frac{\sigma_{Sn}}{\sigma_{Ag}} = 1.71$				$-C_{AgIn} = -31{,}480 + 3.534T - 1.008T\ln(T)$, $L^0 = 542{,}50 - 0.2T + (1.544\text{E}{-8})T\ln(T)$, $L^1 = 110{,}300 - 78.78T - 0.902T\ln(T)$, $L^2 = -29{,}700 + 28.334T + 0.281T\ln(T)$, $\frac{\sigma_{In}\eta_{In}}{\sigma_{Ag}\eta_{Ag}} = 4.52 \pm 0.02 \Rightarrow \frac{\sigma_{In}}{\sigma_{Ag}} = 2.36$			
T (K)	Obtained from the I^+_{Ag}/I^+_{Sn} ratios of this work (Dataset 2 (Run 3))				Obtained from the I^+_{Ag}/I^+_{In} ratios of Miki et al. [4]			
	$-C_{AgSn}$ (intercept)	L^0	L^1	L^2	$-C_{AgIn}$ (intercept)	L^0	L^1	L^2
1273	38880	44570	13000	19920	−37540	43270	43480	21680
1323	39460	37530	22400	15780	−37750	47720	39500	17660
1373	40120	30490	31800	11630	−37970	52170	35510	13630
1423	40780	23450	41200	7491	−38190	56620	31530	9602
1473	41440	16410	50600	3347	−38400	61070	27550	5575
	$-C_{AgSn} = 22{,}000 + 13.2T + (1.668\text{E}{-8})T\ln(T)$, $L^0 = 223{,}800 - 140.8T + (2.39\text{E}{-7})T\ln(T)$, $L^1 = -226{,}300 + 188T - (2.532\text{E}{-7})T\ln(T)$, $L^2 = 125{,}700 - 84.755T + 0.299T\ln(T)$, $\frac{\sigma_{Sn}\eta_{Sn}}{\sigma_{Ag}\eta_{Ag}} = 1.14 \pm 0.04 \Rightarrow \frac{\sigma_{Sn}}{\sigma_{Ag}} = 1.73$				$-C_{AgIn} = -32{,}320 - 2.627T + 0.206T\ln(T)$, $L^0 = (-70{,}027 \pm 0) + (89 \pm 0)T$, $L^1 = (145{,}900 \pm 1400) - (86.0 \pm 8.2)T + (0.77 \pm 0.99)T\ln(T)$, $L^2 = (122{,}900 \pm 1100) - (72.7 \pm 6.4)T - (0.95 \pm 0.78)T\ln(T)$, $\frac{\sigma_{In}\eta_{In}}{\sigma_{Ag}\eta_{Ag}} = 5.09 \pm 0.03 \Rightarrow \frac{\sigma_{In}}{\sigma_{Ag}} = 2.655$			

The *A*, *B* and *C* parameters of the $L(T)$ functions. The numbers behind ± represent standard deviations.

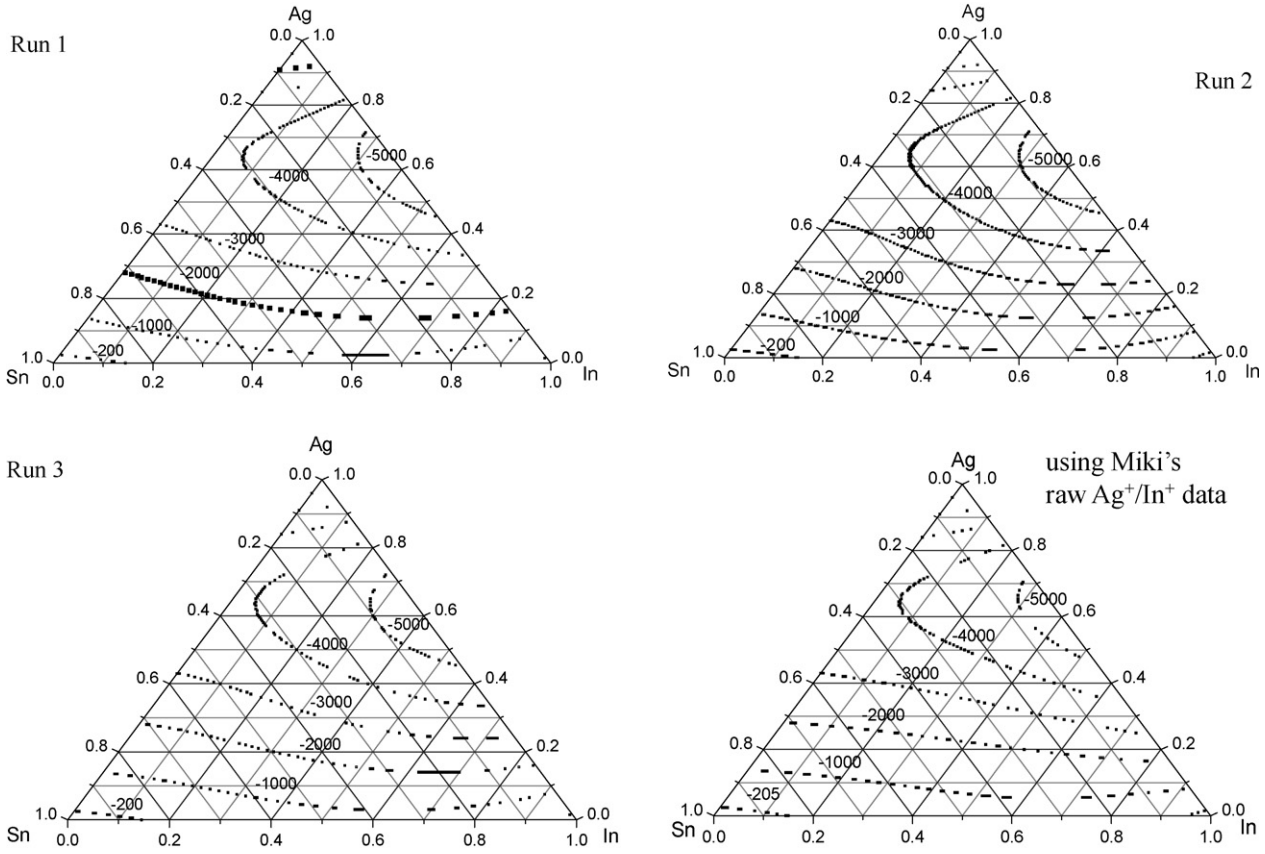

Fig. 5. The iso-excess Gibbs energy curves obtained from Runs 1–3, as well as from Miki et al.'s [4] raw data at 1273 K, using the same binary *L*-parameters from Refs. [16–18]. The values are in J/mol.

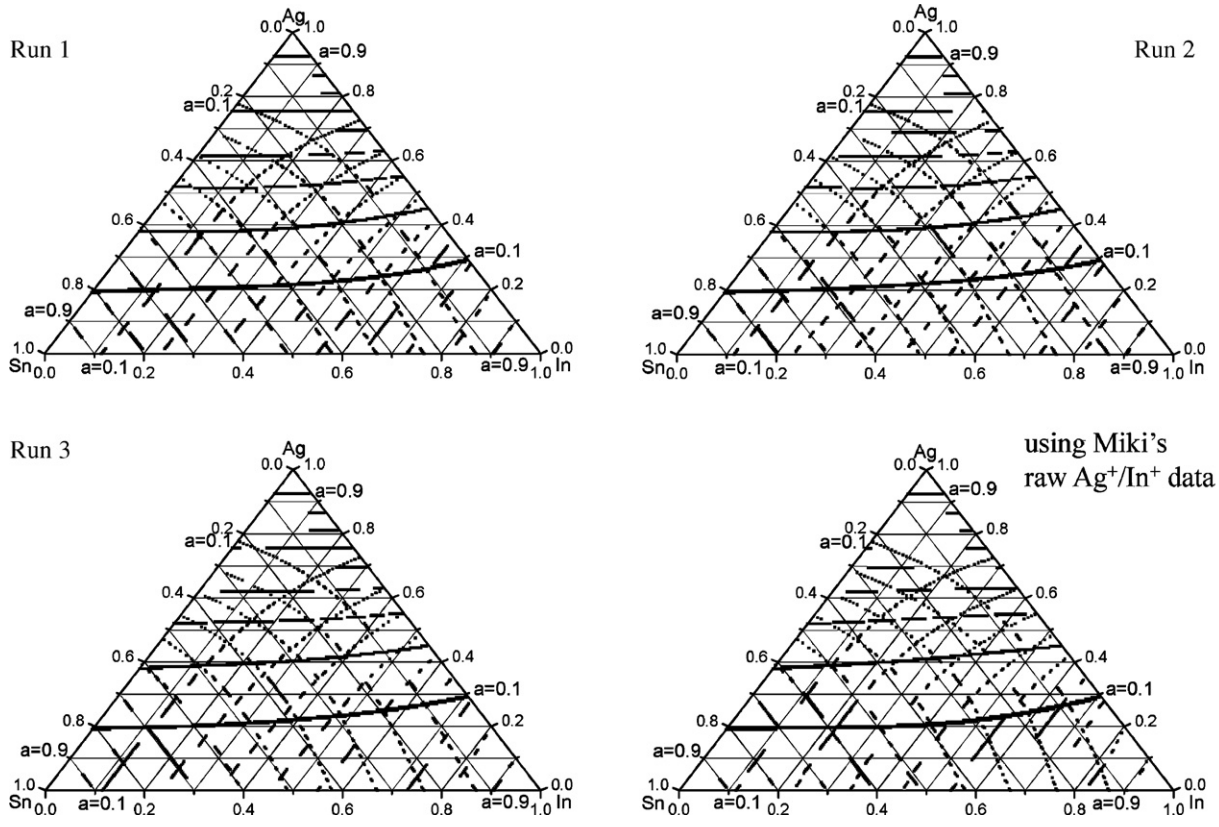

Fig. 6. The iso-activity curves obtained from Runs 1–3, as well as from Miki et al.'s [4] raw data at 1273 K, using the same binary *L*-parameters from Refs. [16–18].

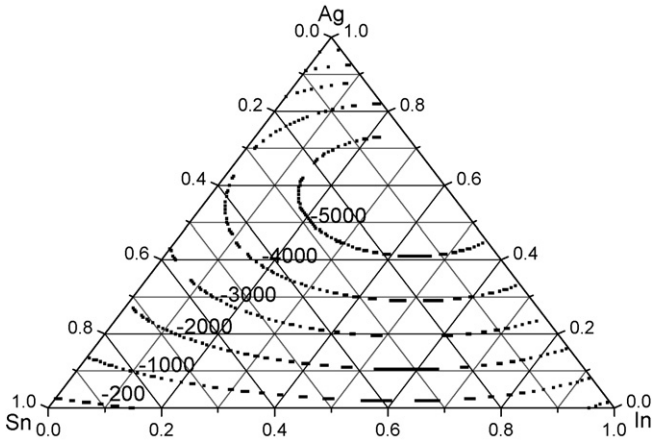

Fig. 7. The iso-excess Gibbs energy curves at 1273 K for Run 2 taking into account binary interactions only.

We have made calculations taking into account only the binary interactions ($L^0_{\mathrm{AgInSn}} = L^1_{\mathrm{AgInSn}} = L^2_{\mathrm{AgInSn}} = 0$) using the raw data of Run 2. The resultant G^{E} data (Fig. 7), and, therefore, also the obtained activity data deviate from the corresponding data presented in Fig. 5 proving that the ternary interaction is not negligible in this system.

We also made RKM calculations using the COST binary *L*-database [21] with both our own KEMS data and Miki et al.'s [4] KEMS data. Fig. 8 shows that the differences between our runs and Miki's G^{E} data are greater when using the COST binary *L*-database [21]. In spite of that the KEMS input data used for making these figures are the same as those for making Fig. 5. Therefore, we strictly relied on the binary *L*'s in Refs. [16–18] rather than those of the COST binary *L*-database [21].

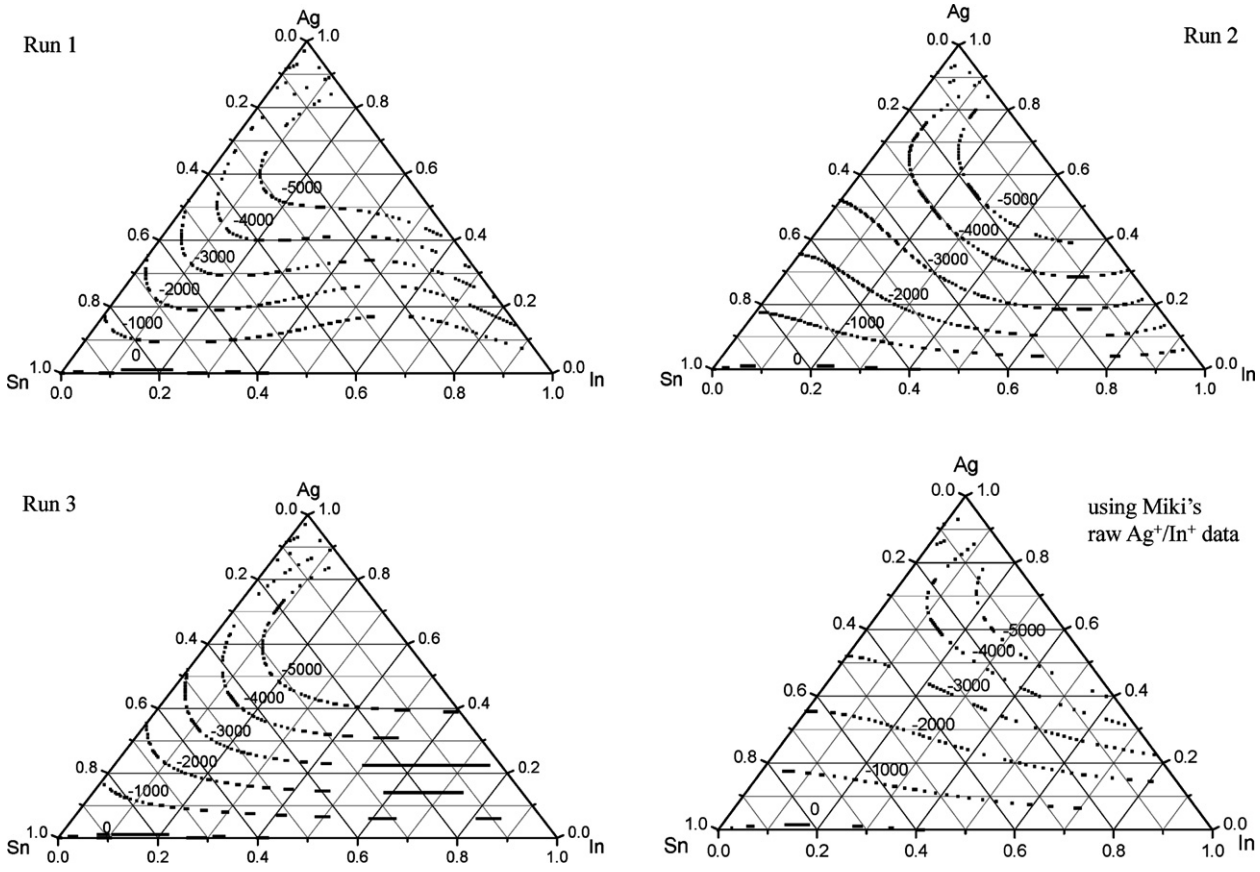

Fig. 8. The iso-excess Gibbs energy curves obtained from Runs 1–3, as well as from Miki et al.'s [4] raw data at 1273 K, using the same COST 531 [21] binary *L*-parameters.

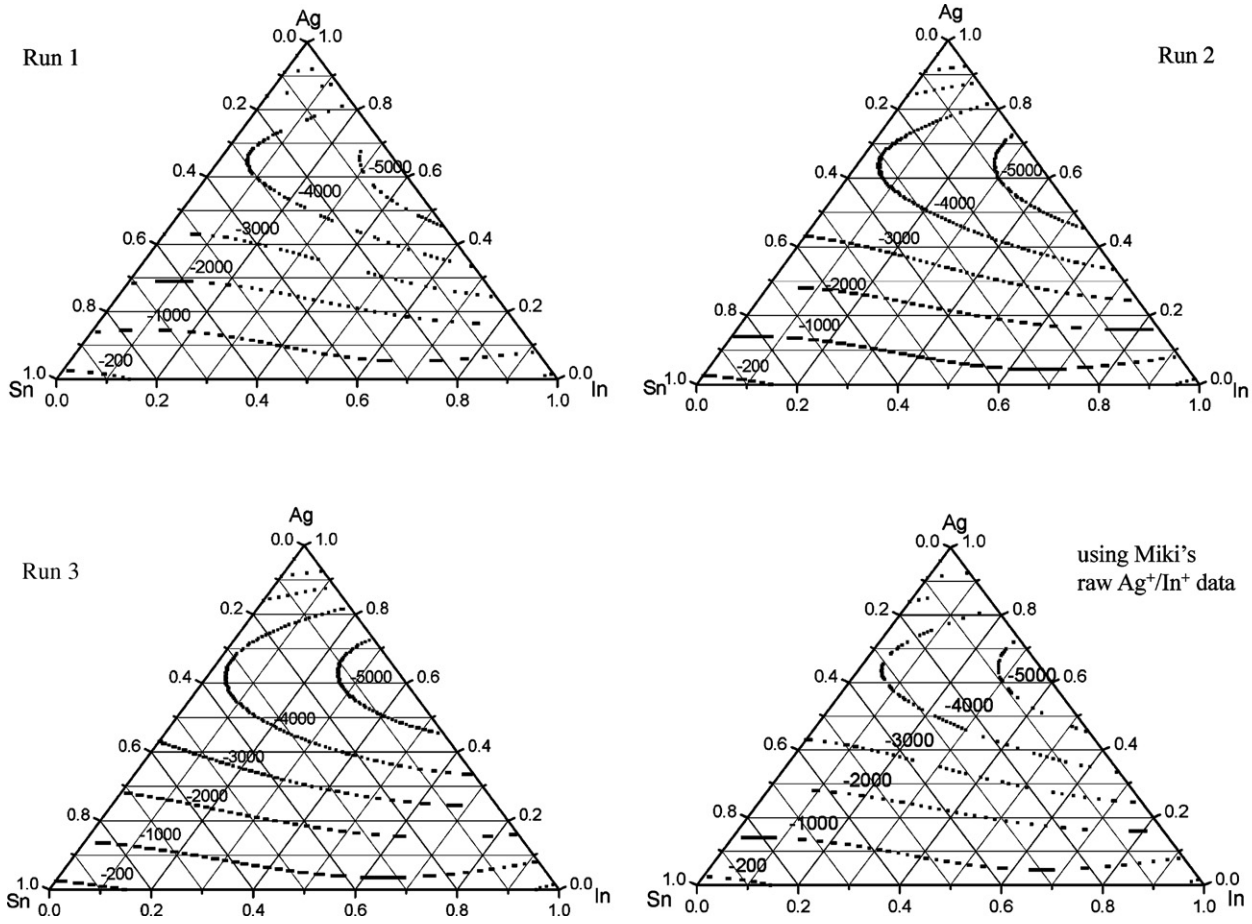

Fig. 9. The iso-excess Gibbs energy curves obtained from Runs 1–3, as well as from Miki et al.'s [4] raw data at 1273 K, modelling the ternary alloy with a single-L and using the same binary L-parameters from Refs. [16–18].

In addition, we have made RKM calculations defining only one-kind of ternary L ($L^0_{\mathrm{AgInSn}} = L^1_{\mathrm{AgInSn}} = L^2_{\mathrm{AgInSn}}$), this is the case in the original paper of Miki et al. [4], but using the same binary L-parameters of Refs. [16–18]. Fig. 9 shows that the differences between our runs and Miki et al.'s [4] G^{E} data are as small as those in Fig. 5. In addition, the values for G^{E} (Fig. 9) are similar to those shown in Fig. 5. Therefore, we conclude that modelling the liquid ternary alloy only with a single ternary L is satisfactory at temperatures of 1273–1473 K. However, this behaviour cannot be generalized since we have proved that the single-L-model was not sufficient to describe the liquid Cu–In–Sn system [6]. The obtained single-L_{AgInSn} values for Ag–In–Sn are as follows:

- Run 1: $L = (55{,}233 \pm 27) - (13.30 \pm 0.02)T$, $L(1273\ \mathrm{K}) = 38{,}300$ J/mol.
- Run 2: $L = (17{,}830 \pm 27) + (11.86 \pm 0.02)T$, $L(1273\ \mathrm{K}) = 32{,}930$ J/mol.
- Run 3: $L = (31{,}422 \pm 27) - (4.66 \pm 0.02)T$, $L(1273\ \mathrm{K}) = 25{,}490$ J/mol.
- From Miki et al.'s [4] raw data: $L = (15{,}924 \pm 27) + (13.86 \pm 0.02)$, $L(1273\ \mathrm{K}) = 33{,}570$ J/mol.

In order to confirm the reliability of the RKM activity data these data were compared to the data obtained by the IEM using Eqs. (23) and (24) in Table 4. The indium activities obtained by the three RKM runs agree with the mean value of the IEM runs using Eq. (23) albeit the IEM runs do not have a very small relative statistical uncertainty. Table 5 gives the results of the IEM experiments. The deviation among the RKM activity values is smaller than the deviation from the IEM data but the latter is still within the uncertainty of the IEM data. The RKM activity values obtained from Miki et al.'s [4] raw data are in agreement with our own RKM data although Miki et al.'s [4] indium activities are the highest of all RKM indium activity data, and, in most cases, they are higher than the corresponding IEM data. The activity of Ag obtained by IEM using Eq. (24) agree well with the RKM data whereas the relative deviation for the Sn data is larger, the relative deviation for the In data is even greater. Nevertheless, this deviation can be caused by a composition shift (distillation) during the two mass loss experiments at the relatively high temperatures (1323 and 1373 K) of these isothermal evaporation experiments (*see* the first two rows in Table 4). The mass loss for these two particular experiments reached higher

Table 4
The activities of certain Ag–In–Sn compositions determined by both IE and RKM methods at the temperatures of the IE experiments

Composition	T (K)	RKM model using Ag^+/In^+ (Run 2)			RKM model using Ag^+/Sn^+ (Run 1)			RKM using model Ag^+/Sn^+ (Run 3)			RKM model using Miki et al.'s Ag^+/In^+ data			IEM (mass loss + mass spectrum or mass loss only)		
		a_{Ag}	a_{In}	a_{Sn}	a_{Ag}	a_{In}	a_{Sn}	a_{Ag}	a_{In}	a_{Sn}	a_{Ag}	a_{In}	a_{Sn}	a_{Ag}	a_{In}	a_{Sn}
$Ag_{0.662}In_{0.117}Sn_{0.221}$	1323	0.466	0.058	0.158	0.465	0.060	0.156	0.462	0.057	0.157	0.459	0.063	0.161	0.436	0.086	0.176
$Ag_{0.45}In_{0.10}Sn_{0.45}$	1373	0.255	0.0725	0.431	0.254	0.0723	0.425	0.247	0.0713	0.435	0.253	0.0823	0.430	0.252	0.120	0.510
$Ag_{0.6}In_{0.2}Sn_{0.2}$	1173	0.366	0.109	0.173	0.370	0.111	0.179	0.366	0.107	0.186	0.348	0.121	0.184	–	0.126 ± 0.015	–
$Ag_{0.4}In_{0.2}Sn_{0.4}$	1173	0.201	0.145	0.406	0.208	0.146	0.406	0.202	0.144	0.432	0.186	0.177	0.432	–	0.131 ± 0.004	–
$Ag_{0.2}In_{0.2}Sn_{0.6}$	1173	0.096	0.157	0.610	0.100	0.156	0.608	0.102	0.159	0.621	0.100	0.190	0.609	–	0.153 ± 0.034	–
$Ag_{0.225}In_{0.100}Sn_{0.675}$	1173	0.111	0.077	0.681	0.114	0.079	0.678	0.116	0.088	0.682	0.112	0.098	0.681	–	0.085	–

The estimated uncertainty of the RKM activity data is below 5%.

Table 5
Isothermal evaporation experiments by measuring the mass loss, and, in some cases, the mass spectrum as well, for several Ag–In–Sn compositions and at different temperatures

Composition	Run	Temperature (K)	Evaporation time (h)	Mass loss (mg)	Mass loss rate (mg/h)	I_{Ag^+} (cps)	I_{In^+} (cps)	I_{Sn^+} (cps)	a_{Ag}	a_{In}	a_{Sn}
$Ag_{0.662}In_{0.117}Sn_{0.221}$	a	1323	11.08	11.1		70390	237480	651	0.436	0.086	0.176
$Ag_{0.45}In_{0.10}Sn_{0.45}$	a	1373	11.58	24.2		139400	1020000	7145	0.252	0.120	0.510
$Ag_{0.6}In_{0.2}Sn_{0.2}$	a	1173	19.55	1.20	0.0614	–	–	–	–	0.136	–
$Ag_{0.6}In_{0.2}Sn_{0.2}$	b	1173	21.80	1.13	0.0518	–	–	–	–	0.115	–
$Ag_{0.6}In_{0.2}Sn_{0.2}$	Mean	1173			0.0566 ± 0.0068	–	–	–	–	0.126 ± 0.015	–
$Ag_{0.4}In_{0.2}Sn_{0.4}$	a	1173	23.47	1.36	0.0580	–	–	–	–	0.129	–
$Ag_{0.4}In_{0.2}Sn_{0.4}$	b	1173	23.35	1.41	0.0604	–	–	–	–	0.134	–
$Ag_{0.4}In_{0.2}Sn_{0.4}$	Mean	1173			0.0592 ± 0.0017	–	–	–	–	0.1314 ± 0.0038	–
$Ag_{0.2}In_{0.2}Sn_{0.6}$	a	1173	23.05	1.61	0.0698	–	–	–	–	0.155	–
$Ag_{0.2}In_{0.2}Sn_{0.6}$	b	1173	21.32	1.78	0.0835	–	–	–	–	0.185	–
$Ag_{0.2}In_{0.2}Sn_{0.6}$	c	1173	21.17	1.12	0.0529	–	–	–	–	0.118	–
$Ag_{0.2}In_{0.2}Sn_{0.6}$	Mean	1173			0.068 ± 0.022	–	–	–	–	0.153 ± 0.034	–
$Ag_{0.225}In_{0.100}Sn_{0.675}$	a	1173	43.18	1.66	0.0384	–	–	–	–	0.085	–

value (11.1 and 24.2 mg) than as mentioned above (2–4 mg relative to 1000 mg sample). Other mass loss experiments performed at 1173 K did not suffer from distillation. The relative ionisation cross-sections (σ) needed for the application of Eq. (24) were obtained by us from the intercepts of the multiple regressions (C_{AgSn}, C_{AgIn} values in Table 3) since the obtained apparent cross-section ratios ($\sigma_{In}/\sigma_{Ag} = 2.36$ (Run 2), $\sigma_{Sn}/\sigma_{Ag} = 1.71$ (Run 1) and $\sigma_{Sn}/\sigma_{Ag} = 1.73$ (Run 3)) usually deviate from the literature cross-sections (Lotz's σ_{In}/σ_{Ag} and σ_{Sn}/σ_{Ag} values are 1.470 and 1.473, respectively, for the same, 30 eV ionising electron energy). This is a frequent phenomenon, *i.e.*, the mass spectra provided by different mass spectrometers can differ due to the different mass discrimination effects in the ion source and detector. This is not a problem when determining activities when applying the IEM using Eq. (24) but the apparent cross-sections provided by the home investigating equipment have to be used in the calculations. Increasing the number of the studied compositions means that the uncertainties of the cross-section ratios obtained by the RKM method will decrease. The σ_{In}/σ_{Ag} values obtained from our and Miki et al.'s [4] device should not be compared because the two devices have different ion source and detector systems. In addition, the value of σ_{In}/σ_{Ag}, obtained from Miki et al.'s [4] measurements, corresponds to an ionising electron energy of 20 eV. The ionisation cross-sections can be determined using the KEMS methods independent of RKM, as well.

Table 6 includes a comparison of the RKM activity data with the data obtained by the Gibbs–Duhem integration. The reference activities selected were those for $Al_{0.45}In_{0.10}Sn_{0.45}$, obtained by the RKM method from the Run 2 measurements whereas the integration were performed using the raw measurements of Ag^+/In^+ and Ag^+/Sn^+ data of Dataset 1. Therefore, the present GD data are not entirely independent of modelling. Table 6 shows an excellent agreement between the GD and RKM data proving that the RKM model must be valid.

4. Reliability of measurements and sources of errors

As can be concluded from the previous chapter, the ternary interaction parameters were obtained using the RKM model, the literature binary *L*-parameters and the KEMS measurements The KEMS measurements were in the present case basically relative measurements, *i.e.*, the ratio of two ion intensities was measured as a function of temperature, in addition to certain model-free KEMS methods (*e.g.*, IEM, GD). There was no need for pressure calibration when making the KEMS measurements in connection with the RKM model, and, therefore no systematic errors originating from the erroneous determination of the instrumental sensitivity appear in the activity values and thermodynamic quantities. The main systematic error concerning in the thermodynamic data originating from RKM model is a result of using literature binary *L*-parameters. It is therefore important to use true (assessed, generally accepted) binary *L*-data. The binary *L*-parameters in Refs. [16–18] proved a more realistic data set than the corresponding COST 531 [21] binary *L*-data. The other source of error (mainly statistical) on the ternary *L*-parameters originates from an insufficient number of compositions. This holds for our three Runs but even so, the uncertainties of the ternary *L*-parameters do not propagate into the values of the activities and excess Gibbs energy. However, for phase diagram calculations, the use of the ternary *L*-parameters obtained from Miki et al.'s [4] raw data is recommended (*see* Eqs. (28)–(30)).

Table 6
The activities of certain compositions determined by both GD and RKM methods at two selected temperatures (at 1273 and 1473 K). The estimated uncertainty of the RKM activity data is below 5%

Compositions of Runs 1 and 2	RKM model using Ag^+/In^+ (Run 2)			RKM model using Ag^+/Sn^+ (Run 1)			RKM model using Ag^+/Sn^+ (Run 3)			RKM model using Miki et al.'s Ag^+/In^+ data			Gibbs–Duhem[a]		
	a_{Ag}	a_{In}	a_{Sn}	a_{Ag}	a_{In}	a_{Sn}	a_{Ag}	a_{In}	a_{Sn}	a_{Ag}	a_{In}	a_{Sn}	a_{Ag}	a_{In}	a_{Sn}
$T = 1273$ K															
$Ag_{0.45}In_{0.10}Sn_{0.45}$	**0.246**	**0.0719**	**0.435**	0.248	0.0740	0.431	0.241	0.0753	0.444	0.240	0.0833	0.443	**0.246**	**0.0719**	**0.435**
$Ag_{0.30}In_{0.10}Sn_{0.60}$	0.154	0.0768	0.603	0.155	0.0777	0.599	0.152	0.0830	0.607	0.152	0.0913	0.604	0.154	0.0794	0.595
$Ag_{0.225}In_{0.10}Sn_{0.675}$	0.114	0.0785	0.678	0.114	0.0789	0.676	0.114	0.0851	0.680	0.115	0.0925	0.676	0.116	0.0770	0.670
$Ag_{0.35}In_{0.30}Sn_{0.35}$	0.175	0.2233	0.362	0.176	0.2346	0.355	0.169	0.2332	0.375	0.167	0.2620	0.376	0.178	0.2246	0.357
$Ag_{0.233}In_{0.30}Sn_{0.467}$	0.112	0.2348	0.479	0.113	0.2451	0.469	0.111	0.2446	0.488	0.115	0.2714	0.478	0.124	0.2583	0.446
$T = 1473$ K															
$Ag_{0.45}In_{0.10}Sn_{0.45}$	**0.264**	**0.0731**	**0.427**	0.260	0.0708	0.420	0.253	0.0681	0.427	0.266	0.0814	0.419	**0.264**	**0.0731**	**0.427**
$Ag_{0.30}In_{0.10}Sn_{0.60}$	0.162	0.0788	0.596	0.158	0.0763	0.592	0.153	0.0770	0.599	0.164	0.0846	0.587	0.161	0.0813	0.595
$Ag_{0.225}In_{0.10}Sn_{0.675}$	0.119	0.0808	0.674	0.115	0.0785	0.672	0.112	0.0805	0.676	0.120	0.0848	0.667	0.120	0.0762	0.678
$Ag_{0.35}In_{0.30}Sn_{0.35}$	0.188	0.2167	0.358	0.179	0.2542	0.338	0.168	0.2649	0.345	0.191	0.2496	0.346	0.196	0.2201	0.347
$Ag_{0.233}In_{0.30}Sn_{0.467}$	0.117	0.2288	0.482	0.114	0.2635	0.455	0.108	0.2742	0.461	0.124	0.2589	0.459	0.136	0.2621	0.431

[a] Reference activities are those of $Ag_{0.45}In_{0.10}Sn_{0.45}$ obtained using RKM on Run 2 data and the calculated activities were obtained using Ag^+/In^+ and Ag^+/Sn^+ data of Dataset 1.

5. Conclusions

Fitting KEMS data to the RKM model was applied and the corresponding mathematical procedure for two ion pair variations (Ag^+/Sn^+ and Ag^+/In^+) was elaborated for the first time without using Miki et al.'s [4] assumption. The obtained Gibbs energy and activity data confirm the mathematical derivations and the consistency of the measurements.

The reliability of the ternary thermodynamic data obtained by fitting KEMS data to the RKM model strongly depends on the input binary *L*-data used. The binary *L*-data taken from Refs. [16–18] proved to be much more realistic than those taken from the COST 531 [21] database.

The obtained RKM activities and excess Gibbs energies agree well with the corresponding data of Miki et al. [4] using the same input binary *L*-data.

The obtained RKM activities and excess Gibbs energies agree very well with the corresponding data obtained using an independent KEMS method (IEM) and a semi-independent KEMS method (GD). Therefore, the RKM model seems to be valid for the liquid Ag–In–Sn alloy.

Though the obtained activities and the excess Gibbs energies are in agreement for all our three runs but the obtained ternary parameters cannot be reproduced due to the high uncertainties caused by the relatively low number of compositions studied. Reliable ternary *L*-parameters can be obtained only from Miki et al.'s [4] raw data.

Assuming only one ternary *L*-parameter ($L^0_{AgInSn} = L^1_{AgInSn} = L^2_{AgInSn} = L_{AgInSn}$ as Miki et al.'s [4] assumption) describes the thermodynamic property of liquid Ag–In–Sn alloy satisfactorily. The reproducibility of this single *L*-parameter obtained from different parallel runs is much better than that of L^0_{AgInSn}, L^1_{AgInSn} and L^2_{AgInSn} and agrees also with Miki et al.'s [4] *L*-value. Nevertheless, in general, the three-parameter-RKM model provides more reliable activity and excess Gibbs energy data than the single-*L*-model.

KEMS is a powerful technique for the determination of thermodynamic activities and Gibbs energy of mixing.

Acknowledgements

The financial support of Slovenian Research Agency is gratefully acknowledged. This work is a contribution to the European COST 531 Action on "Lead-free Solder Materials". Laszlo Bencze wishes to thank for the support to short-term scientific mission trips in the framework of this action. Similarly, our former work resulting in Ref. [6] was also a contribution to the COST 531 Action on "Lead-free Solder Materials" although not acknowledged in the article.

References

[1] H.L. Lukas, J. Weiss, E.-T. Henig, Calphad (1982) 229.
[2] D.W. Marquardt, J. Soc. Ind. Appl. Math. 11 (1963) 431.
[3] E. Königsberger, Calphad 15 (1991) 69.
[4] T. Miki, N. Ogawa, T. Nagasaka, M. Hino, Mater. Trans. 42 (2001) 732.
[5] H. Schmidt, J. Tomiska, J. Alloys Compd. 385 (2004) 126.
[6] A. Popovic, L. Bencze, Int. J. Mass Spectrom. 257 (2006) 41.
[7] B. Gather, P. Schröter, R. Blachnik, Z. Metallkde. 78 (1987) 280.
[8] M. Alaoui-Elbelghiti, Ph.D. Thesis, Rabat, Morocco, 1998.
[9] X.J. Liu, Y. Inohana, Z. Takaku, I. Ohnuma, R. Kainuma, K. Ishida, Z. Moser, W. Gasior, J. Pstrus, J. Electron. Mater. 31 (2002) 1139.
[10] C. Luef, H. Flandorfer, H. Ipser, Metall. Mater. Trans. A 36 (5) (2005) 1273.
[11] J. Drowart, C. Chatillon, J. Hastie, D. Bonnell, Pure Appl. Chem. IUPAC-Tech. Rep. 77 (4) (2005) 683.
[12] A. Popovic, Int. J. Mass Spectrom. 230 (2003) 99.
[13] G.R. Belton, R.J. Fruehan, Metall. Trans. 71 (5) (1967) 1403.
[14] J. Valderrama-N, K.T. Jacob, Thermochem. Acta 21 (1977) 215.
[15] Y.M. Muggianu, M. Gambino, L.P. Bros, J. Chim. Phys. 72 (1975) 85.
[16] T. Yamaji, E. Kato, Metall. Trans. 3 (1972) 1002.
[17] G. Qi, M. Hino, T. Azakami, Mater. Trans., JIM 30 (1989) 575.
[18] B.J. Lee, C.S. Oh, J.H. Shim, J. Electron. Mater. 25 (1996) 983.
[19] G.R. Belton, R.J. Fruehan, Metall. Trans. 1 (4) (1970) 781.
[20] L. Bencze, T. Markus, S. Dash, D.D. Raj, D. Kath, W.A. Oates, W. Löser, K. Hilpert, Metall. Mater. Trans. A 237 (2006) 3171.
[21] A. Kroupa, J. Vřeštál, A. Zemanová, J. Vízdal, A. Watson, A. Dinsdale, Atlas of Lead Free Solders Phase Diagrams, in press.
[22] Z. Moser, W. Gasior, J. Pstrus, W. Zakulski, I. Ohnuma, X.J. Liu, Y. Inohana, K. Ishida, J. Electron. Mater. 30 (2001) 1120.
[23] C.S. Oh, J.H. Shim, B.J. Lee, D.N. Lee, J. Alloys Compd. 238 (1996) 155.
[24] L.N. Ansara, Unpublished result stored within the COST 531 database.